



Interstellar Ices and Radiation-induced Oxidations of Alcohols

R. L. Hudson  and M. H. Moore

Astrochemistry Laboratory, NASA Goddard Space Flight Center, Greenbelt, Maryland, 20771, USA; Reggie.Hudson@NASA.gov

Received 2017 May 2; revised 2018 March 8; accepted 2018 March 9; published 2018 April 18

Abstract

Infrared spectra of ices containing alcohols that are known or potential interstellar molecules are examined before and after irradiation with 1 MeV protons at ~ 20 K. The low-temperature oxidation (hydrogen loss) of six alcohols is followed, and conclusions are drawn based on the results. The formation of reaction products is discussed in terms of the literature on the radiation chemistry of alcohols and a systematic variation in their structures. The results from these new laboratory measurements are then applied to a recent study of propargyl alcohol. Connections are drawn between known interstellar molecules, and several new reaction products in interstellar ices are predicted.

Key words: astrochemistry – infrared: ISM – ISM: molecules – molecular data – molecular processes

1. Introduction

Interstellar ices are now recognized as an important component of the interstellar medium (ISM). The results of multiple infrared (IR) surveys have led to over a dozen assignments of spectral features to molecular ices, with the more abundant interstellar ices being H₂O, CO, and CO₂ (Boogert et al. 2015). Just below these is CH₃OH, methanol, the most abundant interstellar organic ice, and so not surprisingly over the past 30 years the formation and evolution of CH₃OH-ice has been studied by many laboratory astrochemistry groups (e.g., Allamandola et al. 1988; Moore et al. 1996; Palumbo et al. 1999), 2016 alone seeing several new papers (Chuang et al. 2016; Öberg 2016; Saenko & Feldman 2016; Sullivan et al. 2016). Studies have included both the radiolysis (e.g., Hudson & Moore 2000; Bennett et al. 2007) and photolysis (e.g., Gerakines et al. 1996; Muñoz Caro et al. 2014) of solid CH₃OH to understand and predict its interstellar chemistry. All such work on CH₃OH reactions shows that an aldehyde, formaldehyde (H₂CO), is a reaction product of CH₃OH. However, in contrast to the extensive laboratory investigations of CH₃OH stands the paucity of work on other alcohols. This situation is unfortunate as without a set of complementary experiments on other aliphatic alcohols, it is impossible to uncover trends in the chemistry, spectroscopy, and abundances of more-complex alcohol ices and to determine their astrochemical importance.

The need for an exploration of solid-state alcohol chemistry is underscored by the identification of three alcohol-aldehyde pairs in the ISM. The first interstellar organic molecule identified was H₂CO and the second was CH₃OH (Snyder et al. 1969; Ball et al. 1970), which are connected as already mentioned. Another such alcohol-aldehyde interstellar pair is acetaldehyde and ethanol, CH₃C(O)H and CH₃CH₂OH, respectively (Fourikis et al. 1974; Zuckerman et al. 1975). A third combination, perhaps less obvious, is glycolaldehyde and ethylene glycol (Hollis et al. 2000, 2002; Hudson et al. 2005). Relatively little work has been done on such combinations in the solid state except for what has been published for the aforementioned CH₃OH–H₂CO pair.

One of the few other candidate interstellar alcohols that has attracted attention is propargyl alcohol, HC≡C–CH₂OH (Pearson & Drouin 2005). A recent paper in this journal reported new experiments in which a weak, but sharp, peak at

668 cm⁻¹ was produced in solid propargyl alcohol's IR spectrum after the compound was irradiated with 2 keV electrons (Sivaraman et al. 2015, hereafter SMSB from the coauthors final initials). That IR peak was assigned to benzene (C₆H₆), which was said “to be the major product from propargyl alcohol irradiation.” However, a full mid-IR spectrum was shown for only one radiation exposure (~ 30 minutes), with no absorbed dose to compare to that of interstellar ices. The temperature chosen was 86 K and not the 10–20 K usually employed for laboratory experiments with ISM ice analogs. Moreover, the authors' benzene identification was based on an IR peak at 668 cm⁻¹, but the paper cited for support gives 688 cm⁻¹ as benzene's position (Strazzulla & Baratta 1991). Only one reaction product was identified by SMSB, and since no ice thickness or product abundances were included, it is impossible to conclude that benzene, or any other molecule, is “the major product” formed.

The paper of SMSB on propargyl alcohol is a welcome step beyond CH₃OH, but it largely ignores the radiation chemical literature on alcohols of the past 50–60 years and expectations based on molecular structure. For the latter, since propargyl alcohol can be rewritten as X–CH₂OH, where X is H–C≡C–, then it can be considered a substituted version of CH₃OH, and would be expected to produce the corresponding aldehyde on exposure to ionizing radiation.

In the present paper, we first describe new experiments to document a trend in alcohol-ice chemistry, and then we apply that trend to the interesting case of propargyl alcohol. We emphasize that this paper differs from our earlier ones that focus on how various reactants can all lead to the same product, such as a single interstellar ion or molecule (e.g., Hudson et al. 2001; Hudson & Loeffler 2013). This paper also differs from our earlier publications that document the many products that can form from a single reactant or set of reactants (e.g., Hudson & Moore 2000; Hudson et al. 2005). Here we follow a third path by focusing not just on reactants and products, but rather on the type of reaction linking them. We are concerned with a single type of reactant and product and just one region of the mid-infrared spectrum. Our reaction of choice is the oxidation of alcohols to make aldehydes and ketones in interstellar ices. It is not our intent to describe criteria, such as exposure times, for astronomical searches for any of the molecules mentioned, as nearly all of our molecules lack published IR band strengths.

Our goal is an exploration of the connection between alcohols, aldehydes, and ketones in astronomical ices, which has not been attempted since the earliest laboratory astrochemical work on CH_3OH ices (Allamandola et al. 1988).

2. Experimental Methods

All reagents were purchased from Sigma Aldrich and used without additional treatment, other than degassing by freeze-pump-thaw cycles and occasional bulb-to-bulb distillations. Care was taken to avoid unnecessary exposure of propargyl alcohol to sunlight and air, which might have induced the compound's polymerization. Alcohol-containing ices were prepared by vapor-phase deposition onto a pre-cooled (ARS cryostat) substrate inside a vacuum chamber ($\sim 10^{-8}$ torr or better). Depositions were carried out in ~ 1 hr at 9–20 K, and each resulting ice was amorphous.

Ice thicknesses were measured with interference fringes, and were $\sim 1 \mu\text{m}$ in all cases. However, such measurements required a value of the sample's refractive index (n). We adopted $n = 1.30$ for all ices with the exception of propargyl alcohol. None of the results in this paper are influenced by this choice. We measured n at 670 nm for propargyl alcohol using two-laser interferometry as described earlier (e.g., Hudson 2016). Averages of three measurements at 16 K gave $n = 1.26$ with a standard error of ± 0.01 . Room temperature values (Weast 1980) of this alcohol's density (0.9845 g cm^{-3}) and refractive index (1.4322, 590 nm) gave a specific refraction of $0.1817 \text{ cm}^3 \text{ g}^{-1}$ using the Lorentz-Lorenz relation, which when combined with our $n = 1.26$ gave a density of 0.901 g cm^{-3} for propargyl alcohol at 16 K.

Radiation experiments used a polished aluminum substrate, and IR spectra were recorded by reflection off of the sample and underlying substrate. For these experiments, spectra were obtained with a Thermo Nicolet Nexus 670 spectrometer operating at a resolution of 1 cm^{-1} over $5000\text{--}650 \text{ cm}^{-1}$ and with 100 scans per spectrum. This spectrometer and the associated vacuum chamber were interfaced to a Van de Graaff proton accelerator, typically running at a beam current of $1 \times 10^{-7} \text{ A}$ and a proton (p^+) energy of 1.0 MeV, with the integrated beam current being measured in the metal substrate beneath the ice sample. Incident doses measured in this way were on the order of $10^{14}\text{--}10^{15} \text{ p}^+ \text{ cm}^{-2}$. Converting fluences into radiation doses required the sample's stopping power (S), which was calculated with Ziegler's SRIM-2008 program (Ziegler 2008). For propargyl alcohol, we found $S = 252 \text{ MeV cm}^2 \text{ g}^{-1}$ for a 1 MeV p^+ , so that an incident fluence of $1.00 \times 10^{14} \text{ p}^+ \text{ cm}^{-2}$ corresponds to an absorbed dose of 2.34 eV per molecule, which is roughly 403 Mrad or 4.03 MGray. Similar values applied to other alcohols, but were not needed. See Gerakines & Hudson (2013) for details of dose calculations and the many radiation units in common use.

A few IR measurements were made with a second spectrometer (Thermo Nicolet iS50) operating in a standard transmission mode and with settings similar to those already described, but with a KBr substrate. Lab-to-lab comparisons are easier for transmission spectra than for those measured in reflectance due to interference effects from the underlying metal substrate and the choice of angle for incident and reflected IR light. Regardless of the spectrometer used, the IR beam was unpolarized and perpendicular to the plane of the ice.

Our previous publications should be consulted for details and examples of our sample preparation, proton irradiations, dose determinations, and IR spectral measurements (e.g., Moore et al. 2010; Hudson et al. 2017).

3. Results

This paper has two distinct parts. We begin by considering six different alcohols, all proton irradiated near 20 K. The results will be arranged in two different ways to illustrate the influence of molecular structure on the products formed. The six alcohols studied were methanol, ethanol, 1-propanol, 2-propanol, 1-butanol, and *t*-butanol. We generalize from these six compounds to identify one of solid propargyl alcohol's radiation products in a sample that was proton irradiated near 20 K.

3.1. Alcohol Oxidation

Here we demonstrate that ionizing radiation, specifically our 1 MeV proton beam, causes each of our six alcohols to undergo oxidation, which in the present context means loss of hydrogen atoms to form aldehyde molecules and, in one case, a ketone. The hallmark of IR spectra of aldehydes and ketones is a pronounced absorption in the $1800\text{--}1600 \text{ cm}^{-1}$ region, caused by a C=O stretching vibration. Lacking C=O bonds, our alcohols show no significant IR features there, which can be verified by consulting standard references (e.g., Colthup 1950; Pouchert 1997). Therefore, we begin by focusing on the crucial $1800\text{--}1600 \text{ cm}^{-1}$ region.

Figure 1 shows the IR spectra of four straight-chain alcohols, of increasing chain length, after irradiation at 20 K. The uppermost spectrum is from CH_3OH , and the absorption seen near 1722 cm^{-1} has been assigned by Allamandola et al. (1988) and many subsequent authors to H_2CO , formaldehyde. The second spectrum is of irradiated $\text{CH}_3\text{CH}_2\text{OH}$, and the IR peak at 1713 cm^{-1} matches that of solid $\text{CH}_3\text{C(O)H}$, acetaldehyde. The shoulder at 1722 cm^{-1} corresponds to H_2CO . The third spectrum is from 1-propanol. Interestingly, two pronounced peaks, at 1729 and 1695 cm^{-1} , are produced by the radiolysis. The positions and spacing of these peaks match those of $\text{CH}_3\text{CH}_2\text{C(O)H}$, propanal, verified by a reference spectrum of propanal at 20 K that we recorded, the peaks at 1729 and 1695 cm^{-1} being due to a Fermi resonance (Sbrana & Schettino 1970). The bottom spectrum in Figure 1 is from irradiated 1-butanol. The peak and the shoulder at 1714 cm^{-1} and 1699 cm^{-1} , respectively, match positions for $\text{CH}_3\text{CH}_2\text{CH}_2\text{C(O)H}$, butanal (Sbrana & Schettino 1970). Table 1 lists all of these positions and assignments, and a few more to which we return later. Figure 1 demonstrates that irradiation of the four alcohols shown resulted in the oxidation of each of them to the corresponding aldehyde. We emphasize that all of the assignments in Figure 1 were made with the help of reference spectra recorded in our laboratory.

Figure 2 shows a different sequence, this time based on successive substitution of H atoms of CH_3OH by methyl (CH_3) groups. The upper two spectra are copied from Figure 1 and simply alter the carbon chain from CH_3OH to $\text{CH}_3\text{CH}_2\text{OH}$, while the lower two spectra continue the substitution of H by CH_3 . As with Figure 1, ion irradiation of each alcohol ice produced a strong IR absorption in this region, suggesting that each alcohol lost hydrogen and was converted into a compound

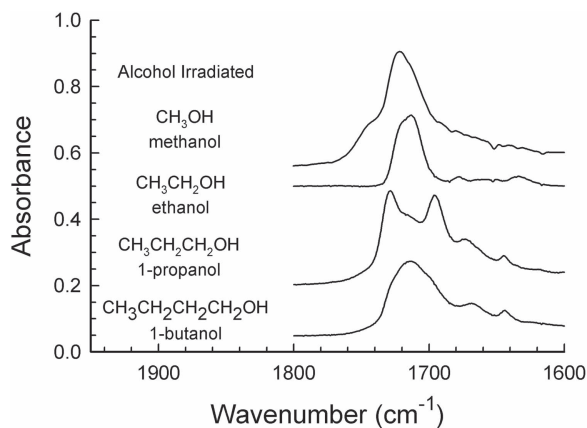


Figure 1. From top to bottom, the carbonyl (C=O) stretching region of the IR spectra of methanol, ethanol, 1-propanol, and 1-butanol. Samples were irradiated at 20 K and held there while IR spectra were recorded. Spectra are offset vertically for clarity. The shoulder near 1743 cm^{-1} is from glycolaldehyde (Hudson et al. 2005).

with a carbonyl (C=O) functional group, again meaning oxidation. It is particularly interesting that irradiated $\text{CH}_3\text{CH}_2\text{OH}$ has products in common with the alcohols above and below it in Figure 2 and that $\text{CH}_3\text{CH}(\text{OH})\text{CH}_3$, 2-propanol, also has products in common with the alcohols placed just above and below it. This trend agrees with expectations, as described in Section 4, and is a powerful argument for the correctness of our interpretation and analysis. Similarly, we expected acetone, $(\text{CH}_3)_2\text{CO}$, to be the only carbonyl-containing product from the irradiation of *t*-butanol and only acetone was found. Table 2 gives peak positions and assignments for Figure 2.

3.2. Propargyl Alcohol Irradiation

Turning to our final alcohol, Figure 3 shows mid-IR transmission spectra of propargyl alcohol deposited at 9 K on a KBr substrate and then warmed to the temperatures indicated. All changes shown were irreversible. The most striking change was at 160–170 K, and was attributable to the crystallization of the initially amorphous solid. Figure 3 represents a routine warming sequence, but it is, to our knowledge, the first time such spectra have been shown for unirradiated propargyl alcohol. Further warming of this same ice to 180 K resulted in its complete sublimation in under a minute in our vacuum system. Similar IR spectra were recorded with the sample deposited on the aluminum substrate used for our radiation experiments. Not only were the two sets of spectra consistent with each other, but they also agreed with literature IR spectra of liquid- and gas-phase propargyl alcohol (Nyquist 1971), the NIST Chemistry WebBook (<http://webbook.nist.gov/chemistry/>), and the Sigma Aldrich atlas (Pouchert 1997). The spectra of Figure 3 were recorded as a control or reference set with which we could distinguish changes caused by thermally induced chemistry from those due to radiation chemistry. These spectra show no evidence for any chemical reactions on warming, such as by changes in the important 1800–1600 cm^{-1} region.

Most of the assignments of propargyl alcohol’s IR bands are straightforward, but one error has crept into the literature and it is important to our work. Each spectrum in Figure 3 shows a sharp peak at $\sim 2121\text{ cm}^{-1}$, which went unassigned by Sivaraman et al. (2015). Their other assignments were taken from Nyquist (1971), who assigned the same peak in

$\text{HC}\equiv\text{C}-\text{CH}_2\text{OH}$ to a $\text{C}\equiv\text{O}$ stretching vibration, which is obviously a typographical error, as the molecule has no $\text{C}\equiv\text{O}$ bonds. The correct assignment for the peak at $\sim 2121\text{ cm}^{-1}$ is a $\text{C}\equiv\text{C}$ vibration.

No attempt was made to determine the IR optical constants of any of our solid alcohols, such as we have done with five nitrile ices (Moore et al. 2010). However, to assist with quantifying our work, and for lab-to-lab comparisons, we measured the apparent absorption coefficients (α') for amorphous propargyl alcohol’s $\text{C}\equiv\text{C}$ and C–C stretching vibrations at 2121 and 914 cm^{-1} , respectively. With data from four ices of different thicknesses, Beer’s law plots (correlation coefficients ≈ 0.997) gave $\alpha'(2121\text{ cm}^{-1}) = 496\text{ cm}^{-1}$ and $\alpha'(914\text{ cm}^{-1}) = 1260\text{ cm}^{-1}$, both for 9 K and with an uncertainty of about 10%. Future work will reduce this uncertainty. See Hudson et al. (2014) and Hudson (2016) for details of α' measurements.

Mid-IR spectra were recorded of irradiated propargyl alcohol ices at both 20 and 85 K, but to a good approximation the results obtained did not depend on the sample’s temperature. Figure 4 presents spectra of a propargyl alcohol ice irradiated at 20 K, the full spectral range being shown so as to compare to the work of SMSB. Figure 5 shows an expansion of the region from 2400 to 1600 cm^{-1} . As with our other six alcohols (Figures 1 and 2), after irradiation, a prominent IR peak appeared in the region due to C=O vibrations, this time at 1664 cm^{-1} . We return to its assignment, and that of the sharp peak growing in at 2100 cm^{-1} , in Section 4. The spectra in Figures 4 and 5 also show that there was a rise in the abundances of CO_2 (2340 cm^{-1}) and, much weaker and at even higher doses, CO (2140 cm^{-1}). Smaller IR changes were seen at lower wavenumbers, but, except for the growth of a weak feature at 950 cm^{-1} , all overlapped with strong bands of the starting material and could not be assigned with confidence. Expansion of the 2000–1900 cm^{-1} region showed two small features that resembled those of allene. Most important of all, no sharp peak for benzene was seen at 600–700 cm^{-1} , although spiking unirradiated propargyl alcohols with benzene ($\sim 5\%$) clearly showed its peak near 688 cm^{-1} . In short, the most obvious IR changes on irradiating propargyl alcohol were the appearance of an intense IR feature at 1664 cm^{-1} , a position consistent with a carbonyl-containing molecule, accompanied by a smaller, but sharp, peak at 2100 cm^{-1} .

This experiment was repeated with several variations, such as at 85 K, at lower doses before warming to search for C_6H_6 , and with H_2O -ice present ($\text{H}_2\text{O}:\text{alcohol} = 20:1$). In all cases, the first and most dramatic spectral change seen was always the appearance of the prominent carbonyl feature near 1664 cm^{-1} . Warming irradiated ices that contained propargyl alcohol gave no evidence of additional chemical change beyond what already has been described. However, an orange-colored residue remained on the metal substrate after an irradiated propargyl alcohol ice was warmed overnight to room temperature under vacuum, and this residue could be removed by repeating washings with ethanol. No such color was seen for the residual material of irradiated $\text{H}_2\text{O} + \text{propargyl alcohol}$ ices. We emphasize that the presence of H_2O -ice, a common interstellar ice component, failed to block the most-prominent spectral changes observed in irradiated propargyl alcohol (Figure 5).

Table 1
Positions and Assignments for Figure 1

Alcohol Irradiated	Formula	Positions of Carbonyl Products (cm^{-1})
Methanol	CH_3OH	1722, H_2CO , formaldehyde
Ethanol	$\text{CH}_3\text{CH}_2\text{OH}$	1713, $\text{CH}_3\text{C}(\text{O})\text{H}$, acetaldehyde, 1722, H_2CO , formaldehyde ^a
1-propanol	$\text{CH}_3\text{CH}_2\text{CH}_2\text{OH}$	1729 and 1695, $\text{CH}_3\text{CH}_2\text{CH}_2\text{C}(\text{O})\text{H}$, propanal, 1722, H_2CO , formaldehyde ^a
1-butanol	$\text{CH}_3\text{CH}_2\text{CH}_2\text{CH}_2\text{OH}$	1714 and 1699, $\text{CH}_3\text{CH}_2\text{CH}_2\text{C}(\text{O})\text{H}$, butanal, 1722, H_2CO , formaldehyde ^a

Note.

^a Somewhat tentative identification from a shoulder in the IR spectrum.

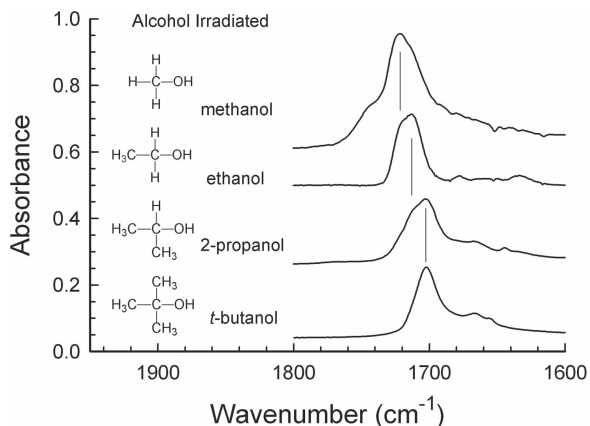


Figure 2. From top to bottom, the carbonyl ($\text{C}=\text{O}$) stretching region of the IR spectra of methanol, ethanol, 2-propanol (isopropanol), and *t*-butanol. Samples were irradiated at 20 K and held there while IR spectra were recorded. Spectra are offset vertically for clarity. The three vertical lines indicate positions of these products: formaldehyde (H_2CO , 1722 cm^{-1}), acetaldehyde ($\text{CH}_3\text{C}(\text{O})\text{H}$, 1713 cm^{-1}), and acetone ($(\text{CH}_3)_2\text{CO}$, 1703 cm^{-1}).

4. Discussion

4.1. Previous Work and Radiation Products

Before starting our experiments, from the radiation chemistry literature, we knew of specific reaction products that were likely to be made in our ices. Work by several groups in the 1950s and 1960s showed that the main products of irradiated alcohols are molecular hydrogen (H_2), a glycol, and an aldehyde (e.g., McDonell & Newton 1955; Meshitsuka & Burton 1958; Dainton et al. 1965). Molecular hydrogen lacks a dipole moment and so is difficult to observe by standard laboratory IR methods, whereas IR spectra of glycols are usually too complex to be unequivocally identified in mixtures. However, aldehydes and ketones possess strong characteristic IR absorbances in the $1800\text{--}1600\text{ cm}^{-1}$ region as was already shown with Figures 1 and 2.

Many publications are available to help explain the radiation products of alcohols, but for this paper only a few reactions are needed. Specifically, Figure 6 shows the formation of the major products of CH_3OH irradiation (Milliken & Johnson 1967) in our work. To reach the main molecular products, two H atoms combine to make H_2 (not shown), and reactions of the hydroxymethyl radical ($\bullet\text{CH}_2\text{OH}$) lead to $(\text{CH}_2\text{OH})_2$, ethylene glycol, by dimerization and to H_2CO by disproportionation. The last reaction in the figure shows how molecular elimination of H_2 from CH_3OH^* also yields H_2CO .

Figure 7 shows the corresponding reactions for ethanol (Williams 1962; Basson 1968; Jore et al. 1988). Here it is the

hydroxyethyl radical ($\text{CH}_3\dot{\text{C}}\text{HOH}$) that will both dimerize to make a glycol, $(\text{CH}_3\text{CHOH})_2$, and disproportionate to make acetaldehyde, $\text{CH}_3\text{C}(\text{O})\text{H}$. Note, however, the added complexity of the last two reactions of Figure 7. The excited $\text{CH}_3\text{CH}_2\text{OH}^*$ can follow two channels of molecular elimination to produce both $\text{CH}_3\text{C}(\text{O})\text{H}$ and H_2CO . Therefore, although the IR spectrum of irradiated CH_3OH shows one aldehyde peak in the 1700 cm^{-1} region, one expects that the IR spectrum of irradiated $\text{CH}_3\text{CH}_2\text{OH}$ will show two IR features, in agreement what is seen in Figures 1 and 2.

Extending these arguments and the reactions of Figures 6 and 7 to our other alcohols is straightforward. One can predict that irradiated 1-propanol will make $\text{CH}_3\text{CH}_2\text{C}(\text{O})\text{H}$ and H_2CO and that irradiated 1-butanol will make $\text{CH}_3\text{CH}_2\text{CH}_2\text{C}(\text{O})\text{H}$ and H_2CO . In both cases, H_2CO is difficult to see in Figure 1, but probably contributes to absorbance in the 1720 cm^{-1} region. Table 1 lists assignments, supported both by literature references and standard samples we prepared at 20 K.

The spectra in Figure 2 illustrate the result of sequentially substituting methyl groups for the three H atoms bonded to the carbon atom in CH_3OH . The products of irradiated CH_3OH and $\text{CH}_3\text{CH}_2\text{OH}$ at the top are H_2CO and $\text{H}_2\text{CO} + \text{CH}_3\text{C}(\text{O})\text{H}$, as already explained. In the third spectrum, the expected products from irradiated 2-propanol are $\text{CH}_3\text{C}(\text{O})\text{H}$ and $(\text{CH}_3)_2\text{CO}$, acetone, and a peak and shoulder are easily seen. For the bottom spectrum, irradiated *t*-butanol can only undergo molecular elimination (of CH_4) to make a single $\text{C}=\text{O}$ containing product, acetone, which is what the peak there matches.

Although the reactions of Figures 6 and 7 account for the most obvious products expected and observed in our irradiated alcohols, other products undoubtedly are present, but will be difficult to detect with low-temperature IR spectroscopy. An example is the six-carbon glycol product expected from the irradiation of propargyl alcohol (vide infra). Such complex molecules might be released on warming an irradiated ice and then detected with mass spectrometry, while other products might only be detectable with room-temperature analyses. In both cases, there could be an ambiguity as to whether the products measured were, in fact, in the ice irradiated at 20 K (or lower) before the sample was warmed.

In addition to the reactions of Figures 6 and 7, processes such as dissociative electron attachment and electron trapping also occur in our experiments, but these lead to no new organic-molecular products that we can easily detect and identify. Also, in some cases, multiple reaction channels can be written, a good example being the second reaction in Figure 6, the dissociation of CH_3OH following the combination of an electron and the radical cation $\text{CH}_3\text{OH}^{+\bullet}$. Three possible

Table 2
Positions and Assignments for Figure 2

Alcohol Irradiated	Formula	Positions of Carbonyl Products (cm^{-1})
Methanol	CH_3OH	1722, H_2CO , formaldehyde,
Ethanol	$\text{CH}_3\text{CH}_2\text{OH}$	1722, H_2CO , formaldehyde, 1713, $\text{CH}_3\text{C}(\text{O})\text{H}$, acetaldehyde
2-propanol	$\text{CH}_3\text{CH}(\text{OH})\text{CH}_3$	1713, $\text{CH}_3\text{C}(\text{O})\text{H}$, acetaldehyde, 1703, $(\text{CH}_3)_2\text{CO}$, acetone
<i>t</i> -butanol	$(\text{CH}_3)_3\text{COH}$	1703, $(\text{CH}_3)_2\text{CO}$, acetone

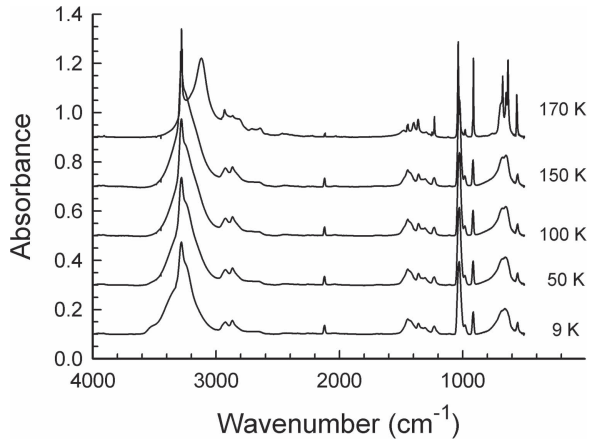


Figure 3. Warming of unirradiated propargyl alcohol from 9 K to the temperatures shown. Spectra have been offset vertically for clarity. These spectra, unlike all others in this paper, were recorded in a standard transmission mode. The thickness of the ice was about $1.6 \mu\text{m}$.

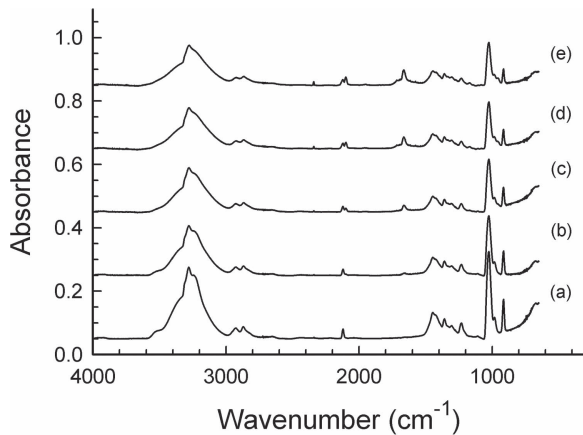
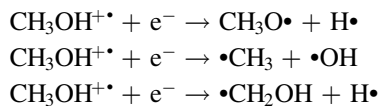


Figure 4. Mid-IR spectra of solid propargyl alcohol at 20 K (a) before irradiation and after irradiation to the following incident fluences: (b) 1.0×10^{13} , (c) 5.0×10^{13} , (d) 1.0×10^{14} , and (e) $1.5 \times 10^{14} \text{ p+cm}^{-2}$.

fragmentations are



where the “ \bullet ” emphasizes the free-radical nature of each product. However, the formation of $\text{CH}_3\text{O}\bullet$, $\bullet\text{CH}_3$, and $\bullet\text{CH}_2\text{OH}$ has been investigated by Toriyama & Iwasaki (1979) who found little or no evidence for either $\text{CH}_3\text{O}\bullet$ or $\bullet\text{CH}_3$ in the electron paramagnetic resonance spectra of CH_3OH glasses irradiated at 4.2 K. Somewhat earlier, it was shown that $\bullet\text{CH}_3$ reacts with CH_3OH in amorphous

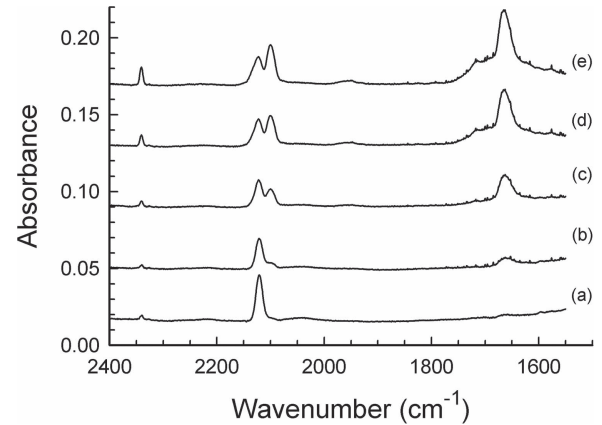


Figure 5. Expansion of Figure 4 from 2400 to 1575 cm^{-1} .

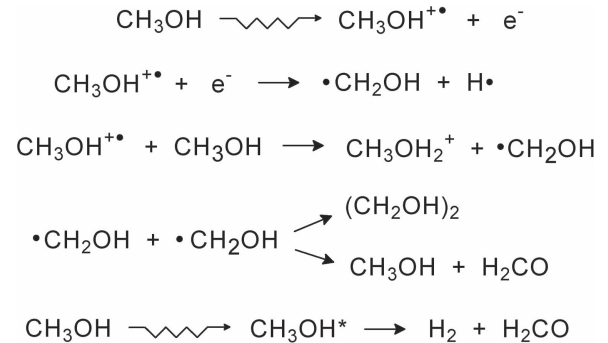


Figure 6. Reactions of irradiated CH_3OH leading to H_2CO , formaldehyde, among other products. Note the two reactions leading to H_2CO : disproportionation and molecular elimination.

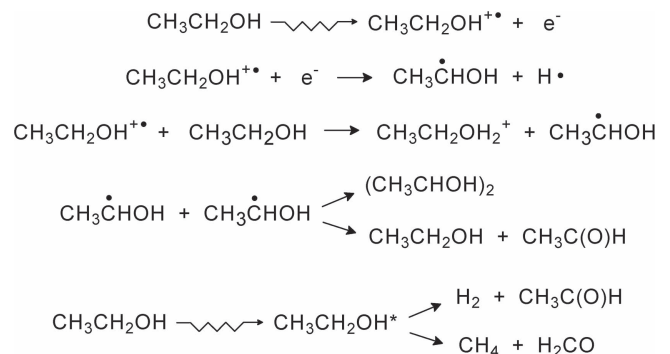


Figure 7. Reactions of irradiated $\text{CH}_3\text{CH}_2\text{OH}$ leading to $\text{CH}_3\text{C}(\text{O})\text{H}$ and H_2CO , acetaldehyde and formaldehyde, respectively, among other products. Note the two reactions leading to $\text{CH}_3\text{C}(\text{O})\text{H}$, disproportionation and molecular elimination, and the one reaction leading to H_2CO .

methanol by

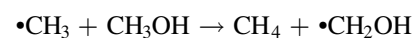


Table 3
Gas-solid Shifts of Carbonyl Peaks in Figures 1 and 2

Molecule	Formula	$\bar{\nu}$ (gas) ^a /cm ⁻¹	$\bar{\nu}$ (solid) ^b /cm ⁻¹	$\Delta\bar{\nu}$ /cm ⁻¹
Formaldehyde	H ₂ CO	1746	1722	24
Acetaldehyde	CH ₃ C(O)H	1743	1714	29
Propanal (propionaldehyde)	CH ₃ CH ₂ C(O)H	1754	1729	25
Acetone	(CH ₃) ₂ CO	1731	1703	28

Notes.

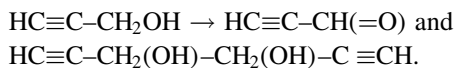
^a Values for H₂CO, CH₃CH(O)H, and (CH₃)₂CO are from Shimanouchi (1972); value for CH₃CH₂C(O)H is from Guirgis et al. (1998).

^b This work; spectra recorded at 20 K.

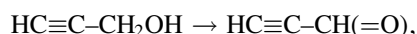
with a temperature-independent half-life near 30 minutes below 40 K, the reaction proceeding by quantum-mechanical tunneling (Hudson et al. 1977). In short, we expect that of CH₃O•, •CH₃, and •CH₂OH, it is the last radical that dominates in our experiments, and will dominate over astronomical timescales in interstellar ices.

4.2. Propargyl Alcohol

Having found good agreement between expectations and observations for the six alcohols of Figures 1 and 2, we now consider our seventh, propargyl alcohol. Reactions similar to those in Figures 6 and 7 can be written to predict this alcohol's two major organic radiation products:



The first product shown is propynal, of the aldehyde family and a known interstellar molecule (Irvine et al. 1988). The second product is a six-carbon glycol, with a complexity that will make it essentially impossible to identify with our methods. Excitation of the parent propargyl alcohol also might give H₂CO as in the case of CH₃OH, CH₃CH₂OH, CH₃CH₂CH₂OH, and CH₃CH₂CH₂CH₂OH in Figure 1. Figures 4 and 5 agree with our expectations for an alcohol-to-aldehyde change. The IR peak appearing 1664 cm⁻¹ on irradiation of propargyl alcohol is assigned to propynal's C=O stretching vibration. A confirmatory peak growing in near 2100 cm⁻¹ with increasing dose is assigned to the molecule's C≡C stretching vibration. The weak feature mentioned earlier near 950 cm⁻¹ is assigned to propynal's C–C stretching vibration. All three assignments are in accord with the work of King & Moule (1961) and the recently published propynal spectrum of Jonusas et al. (2017). These positions are also consistent with those in a room-temperature liquid-phase spectrum of propynal in CCl₄ (Kobayashi & Sumitomo 1972). In short, the most obvious and readily identifiable change in irradiated propargyl alcohol is the conversion from reactant to product according to



as expected from the other alcohols we examined (Tables 1 and 2) and from the literature.

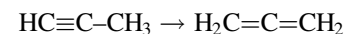
Estimates of the position expected for the C=O band of propynal can also be made from the gas-phase positions of other aldehydes. Table 3 compares gas-phase and solid-phase (our work) positions for three aldehydes and one ketone products, taken from our Tables 1 and 2. The average gas-to-solid shift is

27 cm⁻¹, so from the gas-phase C=O position of 1692 cm⁻¹ for propynal (King & Moule 1961), we predict a solid-phase position of 1692 – 27 = 1665 cm⁻¹, in good agreement with the 1664 cm⁻¹ we observed.

Having established the conversion of propargyl alcohol into propynal, we are faced with estimating the reaction's yield without having either band strengths or optical constants for comparison. The best that we can do is offer a rough value of ~10%, based on similar work we have done with other alcohol-to-aldehyde conversions, primarily ethanol-to-acetaldehyde. We plan to determine and publish optical constants for propynal in the future, which should aid in calculating reaction yields.

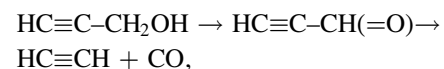
4.3. Other Possible Products

Although the –OH functional group of propargyl alcohol implies that this molecule will undergo chemical changes similar to our other alcohols, propargyl alcohol's alkyne character (HC≡C–) suggests that it also could yield products resembling those of a similar molecule, HC≡C–CH₃, known as propyne or methyl acetylene. Experiments by Jacox & Milligan (1974) demonstrated the ease of a 1,3-H-shift reaction in propyne to give H₂C=C=CH₂, an isomer called allene or 1,3-propadiene. The relevant reaction is

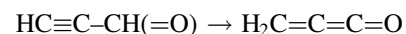


and the strongest IR peak of allene is near 1950 cm⁻¹. After irradiation, our propargyl alcohol samples had two small peaks in the 1950 cm⁻¹ region, probably from H₂C=C=CH₂ (allene) and H₂C=C=CH(OH) (hydroxyallene), but more work is needed to confirm these assignments.

Infrared features of other reaction products could be masked in our spectra by the starting alcohol. For example, the weak CO formation we observed at high doses suggests a sequence such as



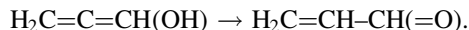
but we have no firm evidence of HC≡CH (acetylene). Similarly, the isomerization



gives propadienone (H₂C=C=C=O), a molecule sought in the ISM (Loomis et al. 2015), but we have no unambiguous evidence for it either.

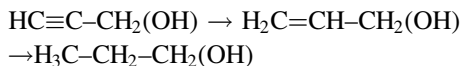
The H₂C=C=CH(OH) already mentioned is an example of a vinyl alcohol. Such species are relatively unstable and undergo a rearrangement known as tautomerism. In this case, rearrangement gives propenal, an interstellar molecule

(Hollis et al. 2004):



Oxidation (hydrogen loss) from the C–C bond of propenal will produce $\text{H}_2\text{C}=\text{C}=\text{C}=\text{O}$, which has already been mentioned.

From studying irradiated $\text{H}_2\text{O} + \text{HC}\equiv\text{CH}$ ices, we also know that triple bonds can be converted into double bonds and single bonds (Hudson & Moore 1997; Moore & Hudson 1998). This implies a similar set of radiation products from propargyl alcohol as



leading to propenol and then to 1-propanol, but again no strong evidence of these products was found. About the only thing that can be said is that several of the spectra in Figures 1 and 2 show weak bumps in the $1700\text{--}1600\text{ cm}^{-1}$ region that might be due to alkenes, vinyl alcohols, or other molecules with C=C bonds. We have not pursued their identification.

Finally, the formation of a refractory solid from irradiated acetylene has long been recognized (Lind et al. 1926; Rasmussen 2017). The resulting material is known as cuprene from the old and now discarded idea that its color indicated that it contained copper. With a sufficient radiation dose to propargyl alcohol, one expects a colored refractory residue to remain afterwards, as we observed. Such a polymeric material could be the result of both free-radical and ionic mechanisms, and might be one of the more abundant radiation products. See Kobayashi & Sumitomo (1972).

From the results presented here, we conclude that the most-prominent radiation-chemical product of amorphous propargyl alcohol observed by IR spectroscopy is propynal, as expected. The most striking spectral changes were the appearance of a pronounced carbonyl peak and a distinct peak from a $\text{C}\equiv\text{C}$ stretching vibration, both corresponding to propynal, an oxidation product. This close correspondence between expectations and observed reaction products argues strongly for the power of predicting ice chemistry from a consideration of molecular structure and literature results. Our work can be extended to other traditional sources of ionizing radiation as well as to the $\text{Ly}\alpha$ lamps typically used by laboratory astrochemists in vacuum-UV photolysis experiments. All are expected to result in the reaction products we observed.

4.4. Comments on Earlier Work

In contrast to the good agreement between expectations and our laboratory results stands our disagreement with the work of SMSB (Sivaraman et al. 2015). None of our experiments produced the sharp feature at 668 cm^{-1} reported by those authors and attributed to benzene. Figure 8 suggests one possible reason for this discrepancy. The upper spectrum was digitized from Figure 1 of SMSB, whereas the lower one was recorded in our laboratory. The lower spectrum agrees with expectations from the literature (Nyquist 1971) and with reference spectra in both the NIST and Aldrich compilations, but the upper spectrum has extra IR bands at $1750\text{--}1600$ and $1550\text{--}1500\text{ cm}^{-1}$. We conclude that the ice that gave the upper spectrum suffered from either a substantial contamination or an experimental artifact, jeopardizing any claim that radiolysis produced IR-detectable amounts of benzene from propargyl alcohol alone. We note that no comparisons to condensed-phase

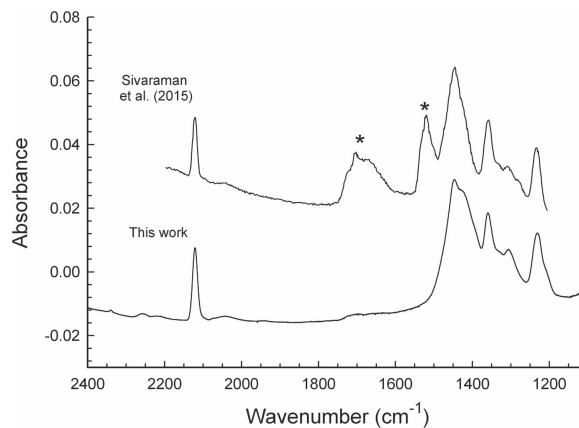


Figure 8. Comparison of the IR spectra of irradiated solid propargyl alcohol from Sivaraman et al. (2015) and from this work. Note the large differences seen at $1800\text{--}1500\text{ cm}^{-1}$ and marked by *. The upper spectrum was digitized from the published version.

spectra were provided. While we cannot say with certainty that benzene was not produced in the work of SMSB, the uncertainty surrounding the starting material (no supplier given), the lack of a connection to the extensive literature on alcohol radiation chemistry, the discrepancy between the observed and literature values for benzene’s IR feature, the lack of explicit attention to reaction chemistry and molecular structure, the missing region of CO_2 ’s strongest IR band, and so on are disconcerting. Somewhat more positively, a close inspection of Figure 1 of SMSB shows a slight increase in absorbance near 2100 and 1664 cm^{-1} after irradiation, the same positions we find for propynal.

5. Some Astrochemical Considerations

For the working astrochemist or astronomer we have shown that the oxidation of an --OH group into a $\text{C}=\text{O}$ group in interstellar ices is not limited to the often-studied $\text{CH}_3\text{OH} \rightarrow \text{H}_2\text{CO}$ conversion, but that it also applies to other alcohols that are known or expected to be interstellar, all reacting to give the corresponding aldehyde or ketone. The 1 MeV proton fluences used in our ice experiments were on the order of $1.5 \times 10^{14}\text{ p+cm}^{-2}$, equivalent to absorbed doses of about $3.5\text{ eV molecule}^{-1}$, roughly the cosmic-radiation dose expected for a dense interstellar cloud over $\sim 10^7$ years (Jenniskens et al. 1993; Moore et al. 2001). Therefore, if an interstellar ice is thought to contain a particular alcohol, then the ice, being exposed to cosmic radiation, should also be considered to harbor the corresponding aldehyde or ketone. Whether these same molecules can be detected in the gas phase depends on, among other things, their sublimation and abundance. Molecular sublimation is fully expected, but remains to be studied in a quantitative way.

We also have shown that according to mid-IR spectroscopy, proton irradiation of amorphous propargyl alcohol gives the aldehyde product expected from a consideration of the literature and the molecular structure of the starting compound. The strongest IR feature appearing after irradiation was from alcohol oxidation, specifically a prominent IR peak that we assign to propynal. In sharp contrast to a recent publication, we found no evidence to support the claim that benzene is a major product of propargyl alcohol radiolysis in a laboratory ice and, by extension, an ice in the ISM, with or without other interstellar ice components present, such as H_2O -ice. From our

new results, one can safely predict that in any interstellar ice in which propargyl alcohol exists, propynal should also be present. However, the degree to which the reverse is true remains to be seen. Radiolytic and photolytic experiments on the low-temperature chemical evolution of propynal and other aldehydes are needed.

For the ice-phase observational astronomer, our Figures 1 and 2 illustrate the difficulty of making firm, unique spectral assignments in the 5.8–5.9 μm ($\sim 1700\text{ cm}^{-1}$) infrared region. The addition of H_2O -ice to alcohol samples could make for more realistic ices, but the situation with regard to the breadth and overlap in the 5.8–5.9 μm region will not improve by the addition of a polar molecule to the alcohols, also polar. For the gas-phase observer, our connection of aldehydes and alcohols suggests that since propanal, propenal, and propynal are known interstellar aldehydes then searches for the corresponding related alcohols 1-propanol, allyl alcohol, and propargyl alcohol, respectively, could be profitable. Similar comments apply to 2-isopropanol (isopropanol), a possible parent of acetone (Combes et al. 1987).

6. Summary and Conclusions

Here we have described new laboratory measurements supporting the generalization of the radiolytic formation of aldehydes and ketones in alcohol-containing ices. Similar results from UV-photolysis experiments are fully expected. Chemical reactions, based largely on the radiation-chemical literature, are described that cover a variety of straight-chained and branched alcohols. The peak positions we tabulate could be useful for searches with IR-capable instruments, such as the *James Webb Space Telescope*, but caution is required in making firm identifications. All of this information constitutes new astrochemical results.

This work was supported by the NASA Astrobiology Institute through funding to the Goddard Center for Astrobiology under proposal 13-13NAI7-0032. Robert Ferrante of the US Naval Academy is thanked for digitizing spectra. Mark Loeffler carried out the radiation experiment with 2-propanol in Figure 2. Perry Gerakines is acknowledged for day-to-day assistance. Lahouari Krim (Université Pierre et Marie Curie) is especially thanked for sharing his propynal results prior to publication. Stephen Brown, Eugene Gerashchenko, and Martin Carts of NASA Goddard's Radiation Effects Facility are thanked for the operation and maintenance of the Van de Graaff accelerator.

ORCID iDs

R. L. Hudson  <https://orcid.org/0000-0003-0519-9429>

References

- Allamandola, L. J., Sandford, S. A., & Valero, G. J. 1988, *Icar*, 76, 225
 Ball, J. A., Gottlieb, C. A., Lilley, A. E., & Radford, H. E. 1970, *ApJL*, 162, L203
 Basson, R. A. 1968, *J. Chem. Soc. A*, 0, 1989
 Bennett, C. J., Chen, S., Sun, B., Chang, A. H. H., & Kaiser, R. I. 2007, *ApJ*, 660, 1588
 Boogert, A. C. A., Gerakines, P. A., & Whittet, D. C. B. 2015, *ARA&A*, 53, 541
 Chuang, K., Fedoseev, G., Ioppolo, S., van Dishoeck, E. F., & Linnartz, H. 2016, *MNRAS*, 455, 1702
 Colthup, N. B. 1950, *JOSA*, 40, 397
 Combes, F., Gerin, M., Wooten, A., et al. 1987, *A&A*, 180, L13
 Dainton, F. S., Salmon, G. A., & Teply, J. 1965, *RSPSA*, 286, 27
 Fourikis, N., Sinclair, M. W., Robinson, B. J., Godfrey, P. D., & Brown, R. D. 1974, *AuJPh*, 27, 425
 Gerakines, P. A., & Hudson, R. L. 2013, *AsBio*, 13, 647
 Gerakines, P. A., Schutte, W. A., & Ehrenfreund, P. 1996, *A&A*, 312, 289
 Guirgis, G. A., Drew, B. R., Gounev, T. K., & Durig, J. R. 1998, *AcSpe*, 54, 123
 Hollis, J. M., Jewell, P. R., Lovas, F. J., Remijan, A., & Møllendal, H. 2004, *ApJL*, 610, L21
 Hollis, J. M., Lovas, F. J., & Jewell, P. R. 2000, *ApJL*, 540, L107
 Hollis, J. M., Lovas, F. J., Jewell, P. R., & Coudert, L. H. 2002, *ApJL*, 571, L59
 Hudson, R. L. 2016, *PCCP*, 18, 25756
 Hudson, R. L., Ferrante, R. F., & Moore, M. H. 2014, *Icar*, 228, 276
 Hudson, R. L., & Loeffler, M. J. 2013, *ApJ*, 773, 109
 Hudson, R. L., Loeffler, M. J., & Yocum, K. M. 2017, *ApJ*, 835, 225
 Hudson, R. L., & Moore, M. H. 1997, *Icar*, 126, 233
 Hudson, R. L., & Moore, M. H. 2000, *Icar*, 145, 661
 Hudson, R. L., Moore, M. H., & Cook, A. M. 2005, *AdSpR*, 36, 184
 Hudson, R. L., Moore, M. H., & Gerakines, P. A. 2001, *ApJ*, 550, 1140
 Hudson, R. L., Shiotani, M., & Williams, F. 1977, *CPL*, 48, 193
 Irvine, W. M., Brown, R. D., Craig, D. M., et al. 1988, *ApJL*, 335, L89
 Jacox, M. E., & Milligan, D. E. 1974, *CP*, 4, 45
 Jenniskens, P., Baratta, G. A., Kouchi, A., et al. 1993, *A&A*, 273, 583
 Jonusas, M., Guillemin, J.-C., & Krim, L. 2017, *MNRAS*, 468, 4592
 Jore, D., Champion, B., Kaouadji, N., Jay-Gerin, J.-P., & Ferradini, C. 1988, *RaPC*, 32, 443
 King, G. W., & Moule, D. 1961, *AcSpe*, 17, 286
 Kobayashi, K., & Sumitomo, H. 1972, *Polymer Lett*, 10, 703
 Lind, S. C., Bardwell, D. C., & Perry, J. H. 1926, *JChS*, 48, 1556
 Loomis, R. A., McGuire, B. A., Shingledecker, C., et al. 2015, *ApJ*, 799, 1
 McDonnell, W. R., & Newton, A. S. 1955, *JChS*, 76, 4651
 Meshitsuka, G., & Burton, M. 1958, *RadR*, 8, 285
 Milliken, S. B., & Johnson, R. H. 1967, *JPhCh*, 71, 2116
 Moore, M. H., Ferrante, R. F., Moore, W. J., & Hudson, R. L. 2010, *ApJS*, 191, 96
 Moore, M. H., Ferrante, R. F., & Nuth, J. A., III 1996, *P&SS*, 44, 927
 Moore, M. H., & Hudson, R. L. 1998, *Icar*, 135, 518
 Moore, M. H., Hudson, R. L., & Gerakines, P. A. 2001, *AcSpe*, 57A, 843
 Muñoz Caro, G. M., Dartois, E., Boduch, P., et al. 2014, *A&A*, 566, 93
 Nyquist, R. A. 1971, *AcSpe*, 27A, 2513
 Öberg, K. I. 2016, *ChRv*, 116, 9631
 Palumbo, M. E., Castorina, A. C., & Strazzulla, G. 1999, *A&A*, 342, 551
 Pearson, J. C., & Drouin, B. J. 2005, *JMoSp*, 234, 149
 Pouchert, C. 1997, *Aldrich Library of FT-IR Spectra* (2nd ed.; Milwaukee, WI: The Aldrich Chemical Company)
 Rasmussen, S. 2017, *Bull. Hist. Chem*, 42, 63, <http://www.scs.illinois.edu/~mainzv/HIST/bulletin/bull17-vol42-1.php>
 Saenko, E. V., & Feldman, V. I. 2016, *PCCP*, 18, 32503
 Sbrana, G., & Schettino, V. 1970, *JMoSp*, 33, 100
 Shimanouchi, T. 1972, *Tables of Molecular Vibrational Frequencies Consolidated*, Vol. I, National Bureau of Standards (Washington, DC: U.S. Government Printing Office)
 Sivaraman, B., Mukherjee, R., Subramanian, K. P., & Banerjee, S. B. 2015, *ApJ*, 798, 72
 Snyder, L. E., Buhl, D., Zuckerman, B., & Palmer, P. 1969, *PhRvL*, 22, 679
 Strazzulla, G., & Baratta, G. A. 1991, *A&A*, 241, 310
 Sullivan, K. K., Boamah, M. D., Shulenberger, K. E., et al. 2016, *MNRAS*, 460, 664
 Toriyama, K., & Iwasaki, M. 1979, *JChS*, 101, 2516
 Weast, R. (ed.) 1980, *CRC Handbook of Chemistry and Physics* (61st ed.; Boca Raton, FL: CRC Press)
 Williams, T. F. 1962, *Natur*, 194, 348
 Ziegler, J. F. 2008, *Stopping and Range of Ions in Matter SRIM2008*, www.srim.org
 Zuckerman, B., Turner, B. E., Johnson, D. R., et al. 1975, *ApJL*, 196, L99